

DO-TH 96/25
February 1997

Limitations of small x resummation methods from F_2 data

I. Bojak and M. Ernst

Institut für Physik, Universität Dortmund
D-44221 Dortmund, Germany

Abstract

We discuss several methods of calculating the DIS structure functions $F_2(x, Q^2)$ based on BFKL-type small x resummations. Taking into account new HERA data ranging down to small x and low Q^2 , we conclude that a pure leading order BFKL-based approach fails to describe the data. Other methods based on high energy factorization are closer to conventional renormalization group equations. Despite several difficulties and ambiguities in combining the renormalization group equations with small x resummed terms, we find that a fit to the current data is hardly feasible, since the data in the low Q^2 region are not as steep as the BFKL formalism predicts. Thus we conclude that deviations from the (successful) renormalization group approach towards summing up logarithms in $1/x$ are disfavoured by experiment.

1 Introduction

Recent measurements of the proton's structure functions [1, 2, 3] have raised the question whether the observed rise of F_2 at small values of x is due to resummation effects described by the BFKL equation [4]. In contrast, this observed rise has already been predicted using the conventional renormalization group equation (RGE) à la Altarelli-Parisi [5] and evolving from a low starting scale [6, 7]. That even data at low Q^2 can be described by the RGE is now widely accepted [8, 9]. So the problem remains if one can find a unique signature in the current F_2 -data for BFKL- or RGE-based evolution equations, or if there is even the possibility of combining the different approaches, aiming at a *unified* evolution equation, which might lead to a better description of the structure function data.

The first question will be dealt with in section 2, where we present an update of our previous work [10] for completeness. This is based on the approach of Askew et al. [11], treating the BFKL-equation as an evolution equation in $\ln 1/x$, and calculating the structure functions from the resulting unintegrated gluon distribution via the k_T -factorization theorem[12, 13].

In section 3 we have a look at the high energy factorization that was developed by Catani et al. [12, 13, 14]. This corresponds to the small x limit, since $s \gg Q^2$ means $x \sim Q^2/s \ll 1$. Based on this work, Forshaw et al. [15] calculated F_2 and F_L by only considering the gluon sector, and by only taking into account small x data ($x < 10^{-2}$). We will show the limitations of this method in section 4.

In section 5 we try to modify the conventional RGE with the complete small x resummed anomalous dimensions of Catani et al., which include also the quark sector in next-to-leading order, as it was already used by Ellis et al. [16]. We will focus on the difficulties of this process, such as caring for energy-momentum conservation, and try to fit the results to the current data, with special emphasis on the low Q^2 data. We supply the details of our previously published results [17] and extend the analysis of the conserving

factors. We will summarize our results in section 6, and comment on the limitations of BFKL inspired calculations of F_2 at relatively low momentum transfers Q^2 .

2 The BFKL equation as an evolution equation

One of the first calculations of small x effects in structure function measurements at HERA was done by Askew et al. [11]. Starting from a gluon ladder diagram in which the transverse momenta are *not* strongly ordered (in contrast to the LO Altarelli-Parisi case), one can infer the BFKL equation, which takes the following form:

$$f(x, k^2) = f_0(x, k^2) + \frac{3\alpha_s}{\pi} k^2 \int \frac{dk'^2}{k'^2} \left[\frac{f(x, k'^2) - f(x, k^2)}{|k'^2 - k^2|} + \frac{f(x, k^2)}{\sqrt{4k'^4 + k^4}} \right]. \quad (1)$$

Note that we deal with the *unintegrated* gluon density $f(x, k^2)$, which is connected to $g(x, Q^2)$ via

$$f(x, k^2) = \left. \frac{\partial x g(x, Q^2)}{\partial \ln Q^2} \right|_{Q^2=k^2}, \quad (2a)$$

$$x g(x, Q^2) = \int_0^{Q^2} \frac{dk^2}{k^2} f(x, k^2). \quad (2b)$$

This is due to the fact that because of the absence of strong ordering the transverse momentum k^2 cannot be integrated out.

Differentiating (1) with respect to $\ln 1/x$ and neglecting the x -dependence of the (non-perturbative) driving term f_0 , we get an evolution equation in x :

$$-x \frac{\partial f(x, k^2)}{\partial x} = \frac{3\alpha_s}{\pi} k^2 \int \frac{dk'^2}{k'^2} \left[\frac{f(x, k'^2) - f(x, k^2)}{|k'^2 - k^2|} + \frac{f(x, k^2)}{\sqrt{4k'^4 + k^4}} \right]. \quad (3)$$

The (approximate) solution of this equation leads to the characteristic small x behaviour of the gluon, with the famous Lipatov exponent λ :

$$f \propto x^{-\lambda}; \quad \lambda = \frac{3\alpha_s}{\pi} 4 \ln 2. \quad (4)$$

Note that the BFKL equation was derived with a *fixed* coupling α_s . We will, however, let the coupling run with k^2 in the following. This has the effect that we get the same

double logarithmic limit as the Altarelli-Parisi equation, and moreover this serves as an effective ultraviolet cutoff.

To make predictions for the structure functions one has to fold the obtain gluon density with the photon-gluon fusion quark box at the end of the ladder via the factorization theorem [12, 13]:

$$F_i^{\text{BFKL}}(x, Q^2) = \int \frac{dk^2}{k^4} \int_x^1 \frac{dy}{y} f\left(\frac{x}{y}, k^2\right) F_i^{(0)}(y, k^2, Q^2), \quad (5)$$

with $i = T, L$ denoting the transverse and longitudinal structure functions, respectively. Explicit expressions for $F_i^{(0)}$ can be found in [18]. Any non-BFKL effects (quark sector, non-perturbative effects) are put into an additional background to Eq. (5). We parametrize it as a soft pomeron, so that F_2 is finally given by

$$F_2(x, Q^2) = F_2^{\text{BFKL}}(x, Q^2) + C_P x^{-0.08}, \quad (6)$$

where the constant C_P is fitted separately for each Q^2 bin.

When starting the evolution at some scale x_0 , it is necessary to continue the gluon distribution somehow into the non-perturbative regime, as the integral in Eq. (3) covers the full range of transverse momenta from zero to infinity. In order to accomplish this, we use the ansatz developed in [11]. It uses several parameters, whose impact on the results was already thoroughly examined in [10]. First of all, there is a scale k_c^2 , below which we use the following ansatz for the gluon distribution that ensures that $f \sim k^2$ for $k^2 \rightarrow 0$:

$$f(x, k^2 < k_c^2) \sim \frac{k^2}{k^2 + k_a^2} f(x, k_c^2). \quad (7)$$

The proportionality constant is chosen so that f is continuous at $k^2 = k_c^2$. Additionally, the input gluon at $x = x_0$ is shifted by k_a to soften the infrared behaviour:

$$f(x_0, k^2) \longrightarrow f(x_0, k^2 + k_a^2). \quad (8)$$

A similar shift is applied to the strong coupling constant:

$$\alpha_s(k^2) \longrightarrow \alpha_s(k^2 + k_b^2). \quad (9)$$

We avoid to repeat a detailed discussion of the parameters, but want to sum up the key features of this approach:

- The results depend only in a minor way on the given parameters k_b^2 , k_c^2 , which should be about 1 GeV².
- The impact of k_a^2 is much stronger; however, this parameter is fixed by the consistency constraint that the integrated input gluon distribution should match the original gluon g at medium to high Q^2 via Eq. (2b). This leads to the following relation:

$$\ln \frac{k_c^2 + k_a^2}{k_a^2} \approx \frac{x_0 g(x_0, k_c^2 + k_a^2)}{f(x_0, k_c^2 + k_a^2)}. \quad (10)$$

For a MRS D_0 -type gluon [19] we obtain $k_a^2 = 0.95$ GeV², but the GRV '92-LO gluon [7] for example implies a low $k_a^2 = 0.19$ GeV² [10].

- As a consequence, only “old” gluons (e.g. MRS D_0 and D_- [19]) can be used; newer gluon inputs (with low k_a^2) generate structure functions which are much too steep.

Using the D_0 -type gluon [19], we calculated the structure function F_2 , and compared it to the available HERA data [2, 3] as well as E665 data [20]. After fitting the background contribution in Eq. (6), we obtain the solid curves in Fig. 1. The dashed curves show the background contribution. For $Q^2 = 3.5$ GeV² and $Q^2 = 6.5$ GeV² the background would be *negative* and is therefore set to zero.

We see that agreement with the data only gets acceptable for Q^2 large ($\chi^2/\text{d.o.f.}=1.3$ for $Q^2 = 65$ GeV²), but even there the conventional description is better. For lower Q^2 , the obtained $\chi^2/\text{d.o.f.}$ can get as high as 27 ($Q^2 = 6.5$ GeV²). The BFKL evolution generates slopes which are almost independent of the Q^2 bins under consideration. But it is too steep for most of the data points, especially in the lower Q^2 bins. Conventional RGE calculations seem to be more flexible in this respect. We will have a closer look at the slope in section 6. So we conclude that this whole procedure is now definitely ruled out by the new data, due to their precision and their flatness in the lower Q^2 region.

3 High energy k_T -factorization

Another method of summing small x logarithms was proposed by Catani et al. [13, 14]. It is based on the high k_T -factorization, which has the advantage of being compatible with the conventional collinear factorization. We just want to present the basic outline, without going into details. First, we define the renormalization group equations in Mellin space:

$$f_i(n, Q^2) = \sum_j \gamma_{ij} f_j(n, Q^2). \quad (11)$$

Our interest now focuses on the quark singlet combination $f^s \equiv x \sum_{i=1}^{N_f} (q_i + \bar{q}_i)$ and the gluon density $f^g \equiv xg$. Note that we have rescaled the parton distribution by x for convenience. This implies that the anomalous dimensions are connected to the x -space splitting functions \mathcal{P}_{ij} via

$$\gamma_{ij}(n) = \int_0^1 x^n \mathcal{P}_{ij}(x) dx = \mathcal{P}_{ij}(n+1), \quad (12)$$

which differs by one from the standard definition. These anomalous dimensions are in conventional perturbation theory given as a power series in α_s , of which the first two orders are known today.

With the method of Catani et al., we are now looking for corrections to the anomalous dimensions and coefficient functions of the form α_s^{i+k}/n^k . Up to now, these have been calculated for $i = 0$ to all orders in α_s/n , and partially for $i = 1$. The singularities in moment space ($n \rightarrow 0$) correspond to the small x limit in x -space.

The corrections to the gluon anomalous dimension can be inferred from the solution of the characteristic equation ($\bar{\alpha}_s = C_A \alpha_s / \pi$; for QCD $C_A = 3$, $C_F = 4/3$, $T_R = 1/2$):

$$\bar{\alpha}_s \chi(\gamma_L) = n; \quad \chi(\gamma) = 2\psi(1) - \psi(\gamma) - \psi(1 - \gamma). \quad (13)$$

For $z \equiv \bar{\alpha}_s/n$ small, this solution can be written as a power series in z :

$$\gamma_L(z) = z + 2\zeta(3)z^4 + 2\zeta(5)z^6 + \mathcal{O}(z^7). \quad (14)$$

The coefficients of this power series can be calculated to arbitrary orders; a list of the first 14 is given for example in the first reference of [14]. There is a branching point in the solution for $n_r = 4\bar{\alpha}_s \ln 2$, corresponding to $\gamma_L = 1/2$. This branching point is again the Lipatov exponent, which governs the small x behaviour of the gluon distribution (and the structure function), as we have already seen in the previous section. The gluonic small x resummed anomalous dimensions can then be expressed as

$$\gamma_{gg} = \gamma_L; \quad \gamma_{gq} = \frac{C_F}{C_A} \gamma_L. \quad (15)$$

The quark sector only contributes in the next-to-leading order, introducing an additional factorization scheme dependence in the expressions. Furthermore, one has not yet found a simple closed expression for the quark anomalous dimensions like Eq. (13). In the $\overline{\text{MS}}$ -scheme for example, the power series begins like [13]:

$$\gamma_{NL} = \frac{\alpha_s}{2\pi} T_R \frac{2}{3} \left\{ 1 + \frac{5}{3}z + \frac{14}{9}z^2 + \mathcal{O}(z^3) \right\}. \quad (16)$$

The calculation of the coefficients is much more involved than in the leading order case; numerical expressions for the first 18 coefficients can be found for example in [15]. Note that while γ_L has its first correction in 4-loop-order (Eq. (14)), γ_{NL} has corrections in *every* order. We get γ_{qq} and γ_{qg} from the following relation:

$$\gamma_{qq} = \frac{C_F}{C_A} \left(\gamma_{NL} - \frac{\alpha_s}{2\pi} T_R \frac{2}{3} \right); \quad \gamma_{qg} = \gamma_{NL}. \quad (17)$$

With these corrections γ_L , γ_{NL} the singlet small x anomalous dimension matrix can then be written as follows:

$$\hat{\gamma} = \begin{pmatrix} 0 & 0 \\ \frac{C_F}{C_A} \gamma_L & \gamma_L \end{pmatrix} + \begin{pmatrix} 2N_f \frac{C_F}{C_A} (\gamma_{NL} - \frac{\alpha_s}{2\pi} T_R \frac{2}{3}) & 2N_f \gamma_{NL} \\ \gamma_\delta & \gamma_\eta \end{pmatrix} + \mathcal{O} \left(\alpha_s^2 \left(\frac{\alpha_s}{n} \right)^k \right), \quad (18)$$

where γ_δ , γ_η denote the yet unknown next-to-leading order gluonic contributions. Note that the non-singlet part of the renormalization group equation is not affected by small x contributions as singular as γ_L , γ_{NL} .

This discussion is not complete until we mention how to compute physical observables such as structure functions within this framework. It is possible to obtain appropriate

coefficient functions to the same accuracy as the anomalous dimensions given above. Concerning F_2 , one can calculate its scaling violations in n -moment space in the limit $n \rightarrow 0$ from the gluon distribution via the following expression ($\langle e^2 \rangle$ denotes the mean squared electric charge of the involved quarks):

$$\frac{dF_2}{d \ln Q^2} = \langle e^2 \rangle (C_2^g \gamma_{gg} + 2N_f \gamma_{qg}) f^g \quad (19)$$

$$= \langle e^2 \rangle h_2(\gamma_L) R_n(\gamma_L) f^g \quad (20)$$

The function h_2 is basically the Mellin-transform of the off-shell cross section $d\hat{\sigma}/d \ln Q^2$, whereas R_n is a process-independent, but (in general) factorization scheme dependent renormalization factor. They are given by [13]

$$\begin{aligned} h_2(\gamma) &= \frac{\alpha_s}{2\pi} N_f T_R \frac{2(2+3\gamma-3\gamma^2)}{3-2\gamma} \frac{\Gamma^3(1-\gamma)\Gamma^3(1+\gamma)}{\Gamma(2-2\gamma)\Gamma(2+2\gamma)} \\ &= \frac{\alpha_s}{2\pi} N_f T_R \frac{2(2+3\gamma-3\gamma^2)}{3-2\gamma} \left(\frac{\pi^2 \gamma^2}{1-4\gamma^2 \sin(\pi\gamma) \tan(\pi\gamma)} \right) \end{aligned} \quad (21)$$

and

$$\begin{aligned} R_n(\gamma) &= \left\{ \frac{\Gamma(1-\gamma)\chi(\gamma)}{\Gamma(1+\gamma)[- \gamma \chi'(\gamma)]} \right\}^{\frac{1}{2}} \times \\ &\times \exp \left\{ \gamma \chi(1) + \int_0^\gamma d\gamma \frac{\psi'(1) - \psi'(1-\gamma)}{\chi(\gamma)} \right\}. \end{aligned} \quad (22)$$

This can also be expanded in powers of $z \equiv \alpha_s/n$:

$$R_n = 1 + \frac{8}{3} \zeta(3) z^3 - \frac{3}{4} \zeta(4) z^4 + \mathcal{O}(z^5). \quad (23)$$

With these expressions it is possible to calculate the Wilson coefficient C_2^g to the same precision as γ_{qg} via Eq. (19). In the $\overline{\text{MS}}$ -scheme we get

$$C_2^g = \frac{\alpha_s}{2\pi} N_f T_R \frac{2}{3} \left\{ 1 + 1.49z + 9.71z^2 + 16.43z^3 + \mathcal{O}(z^4) \right\} \quad (24)$$

Again, more coefficients in this power series have been calculated in [15].

If we turn to the DIS factorization scheme, some expressions become a bit simpler. In fact, since this scheme is defined by the requirement for the Wilson coefficients $C_2^g = 0$, $C_2^q = 1$, the quark anomalous dimension simply becomes

$$2N_f \gamma_{qg} = h_2(\gamma_L) R_n(\gamma_L) \quad (25)$$

(cf. Eq. (19)). Fortunately, the expression for R_n remains the same (Eq. (22)), and as γ_L is per definition scheme independent, we can obtain fully resummed expressions in the gluon *and* quark sector. A drawback is that the coefficients for γ_{qg} become larger, especially at large orders; the first terms read

$$\gamma_{qg}^{\text{DIS}} = \frac{\alpha_s}{2\pi} T_R \frac{1}{3} \left\{ 1 + 2.17z + 2.30z^2 + 8.27z^3 + \mathcal{O}(z^4) \right\}. \quad (26)$$

4 Gluon based approach

After this introduction to the formalism, we will focus on its implications on the description of the measured structure function data. Our first example is the approach developed by Forshaw et al. in [15]. The basic idea is to use *only* the LO small x contributions γ_L in the anomalous dimension matrix (18), so that the quark singlet part is decoupled from the gluon and moreover not evolved at all. The Altarelli-Parisi equation then reduces to this simple expression

$$\frac{df^g(n, Q^2)}{d \ln Q^2} = \frac{C_F}{C_A} \gamma_L f^s(n, Q^2) + \gamma_L f^g(n, Q^2) \quad (27)$$

with the equally simple solution

$$f^g(n, Q^2) = \left[\frac{C_F}{C_A} f^s(n, Q_0^2) + f^g(n, Q_0^2) \right] \exp \left(\int_{Q_0^2}^{Q^2} \frac{dk^2}{k^2} \gamma_L \right) - \frac{C_F}{C_A} f^s(n, Q_0^2). \quad (28)$$

This will be further simplified by completely neglecting the quark singlet $f^s(n, Q_0^2)$ because of the expected gluon dominance in the small x regime.

Following the argumentation of the previous section, we can include the renormalization factor R_n into the gluon distribution before calculating structure functions:

$$G(n, Q^2) = R_n f^g(n, Q^2) = R_n Z_n(Q^2, Q_0^2) f^g(n, Q_0^2) \quad (29)$$

with

$$Z_n(Q^2, Q_0^2) = \int_{Q_0^2}^{Q^2} \frac{dk^2}{k^2} \gamma_L. \quad (30)$$

If we want to transform this back into x -space, we have to perform the following complex integral:

$$G(x, Q^2) = \frac{1}{2\pi i} \int_C dn x^{-n} R_n f^g(n, Q_0^2) \exp[Z_n(Q^2, Q_0^2)], \quad (31)$$

The integration contour C lies as usual to the right of all singularities in the complex n -plane. However, in this approximation we notice that the factors R_n and Z_n only have one singularity for $n = 0$, when we use the appropriate series expansions of γ_L and R_n (Eqs. (14) and (23)). If now the gluon input $f^g(x, Q_0^2)$ is chosen as a simple step function [15],

$$f^g(x, Q_0^2) = \mathcal{N} \theta(x_0 - x) \implies f^g(n, Q_0^2) = \mathcal{N} \frac{x_0^n}{n}, \quad (32)$$

with a suitably chosen x_0 , there is no other singularity at all, and the integration contour in Eq. (31) can be chosen as a circle around the origin. Now it is possible to find an analytic solution to the integral as a series of Bessel functions [15]:

$$\begin{aligned} G(x, Q^2)/\mathcal{N} &= \sum_{i=0}^{\infty} c_i \left(\frac{\xi}{\gamma^2 \zeta} \right)^{i/2} I_i(2\sqrt{\gamma^2 \xi \zeta}) \\ &+ \sum_{i=0}^{\infty} \sum_{j=2}^{\infty} c_i b_j \left(\frac{\xi}{\gamma^2 \zeta} \right)^{(i+j)/2} I_{i+j}(2\sqrt{\gamma^2 \xi \zeta}) \\ &+ \sum_{i=0}^{\infty} \sum_{j=2}^{\infty} \sum_{k=2}^{\infty} \frac{c_i b_j b_k}{2} \left(\frac{\xi}{\gamma^2 \zeta} \right)^{(i+j+k)/2} I_{i+j+k}(2\sqrt{\gamma^2 \xi \zeta}) + \dots \end{aligned} \quad (33)$$

Here we employed the following abbreviations:

$$\zeta = \ln \frac{\alpha_s(Q_0^2)}{\alpha_s(Q^2)}, \quad \xi = \ln \frac{x_0}{x}, \quad \gamma^2 = \frac{12}{\beta_0}, \quad (34)$$

and the coefficients c_i , b_i are those of the series expansions of R_n and Z_n , respectively.

In order to form the structure function F_2 , one further integration according to Eqs. (19) and (20) has to be done. Since all the relevant quantities can in the same way be expressed as a power series like R_n , we only need to replace the coefficients c_i by the appropriate ones to obtain the right hand sides of Eqs. (19) and (20). While these equations are equivalent to leading order, Forshaw et al. proposed to include the

derivative of the coefficient function $\partial C_2^g / \partial \ln Q^2$ upon integration, although it is formally subleading in Eq. (19), since it may lead to contributions which are not negligible.

The missing input $F_2(x, Q_0^2)$ has been parametrized as $A + Bx^{-\lambda}$, introducing three additional parameters. In [15], x_0 was set to 0.1, and a (remarkably) low $\Lambda_{\text{QCD}}^{(4)}$ of 115 MeV was chosen. This leaves five parameters ($Q_0^2, \mathcal{N}, A, B, \lambda$) free to be fitted against structure function data. Using 1993 data [2] below $x = 0.01$, they obtain a very good χ^2 , which is slightly better when the subleading terms mentioned above are included. It was our intention to test whether this approach still works for more recent data, which are more precise, and which especially extend down to lower Q^2 .

4.1 Fits using the analytic formulae

Our first observation is that the excellent agreement with the data in [15] does not last very long. Let us first note that the variable ζ becomes ill-defined for $Q^2 < Q_0^2$. This implies that in order to describe the low Q^2 data, one has to choose at least an equally low Q_0^2 . This already worsens the χ^2 for the 1993 data slightly (but it is still acceptable). If we now include the 1994 HERA data and the E665 data, the situation gets much worse, see table 1 for details. As in [15], we set $x_0 = 0.1$, and only used data with $x < 0.01$. One can see that the fits including the subleading terms are in principle better than those without. Nevertheless, the χ^2 of all these fits is not very convincing. It is better, the higher we chose Q_0^2 , so we focus in the following on $Q_0^2 = 2 \text{ GeV}^2$.

As is visible in Fig. 2, the agreement with the data is not very good. The inclusion of the subleading terms (solid line) leads to curves which are “bent” down to the negative region for very small x . It is obvious that for these values of x this approach is not reliable anymore, as was already seen in [15], too. With the 1993 data, this was not an issue, as there were no data in this kinematic region. But with the new data, this becomes a problem. Regarding the other curve without the subleading terms (dashed line), agreement with data is better, but we see also that the influence of $F_2(Q_0^2)$ is bigger:

Q_0^2 [GeV ²]	data points	\mathcal{N}	A	B	λ	χ^2
0.8	257	0.74	0.21	$0.65 \cdot 10^{-3}$	-0.94	650
without subl. terms		0.41	0.42	-0.024	-0.71	900
1.0	250	0.80	0.23	0.0018	-0.79	478
without subl. terms		0.51	0.47	-0.0066	-0.57	646
2.0	232	1.1	-0.032	0.12	-0.26	337
without subl. terms		0.71	0.44	$0.48 \cdot 10^{-20}$	-4.68	307
2.0	232	0.39	-2.40	2.02	-0.076	1502

Table 1: Parameters for various fits to F_2 data. In last row $\Lambda_{\text{QCD}}^{(4)} = 177$ MeV.

The gluon normalization \mathcal{N} is smaller, and the parameters B and λ acquire almost absurd values.

The next question which arises concerns Λ_{QCD} . It is clear that this has a serious impact on the calculation, since the value of α_s controls γ_L and thus the steepness of the gluon and the structure function. We tried to use a more realistic value of $\Lambda_{\text{QCD}}^{(4)} = 177$ MeV. This leads to an even stronger disagreement with the data. Moreover, relative to the other curves, the influence of the input $F_2(x, Q_0^2)$ is stronger, \mathcal{N} being even smaller. This leads to the conclusion that the fitting procedure tries to reduce the influence of the (BFKL driven) gluon. To summarize, this simple analytic approach is disfavoured by the recent data. Note again that these data can be well described by a conventional renormalization group analysis.

However, there remains one way out: If we abandon the simple step function like input gluon density, then the situation may be improved. It was already noted in [15], that the analytic formula Eq. (33) could be extended to more complex input densities. Unfortunately, we find this not to be the case: In the first place, one has to choose an ansatz whose Mellin transform has a *finite* number of n -plane singularities. This means e. g. for a standard gluon input of the form

$$f^g(x, Q_0^2) \sim x^\alpha (1-x)^\beta, \quad (35)$$

which transforms into a Beta-function, that either α or β have to be integer. While this is not too strong a constraint, the next problem arises immediately: For the analytic inversion it is essential that the input can be written as a power series in $1/n$. However, the Laurent series stemming from Eq. (35) does *not* converge. Apart from that, one has to take into account that the expense of performing a fit based on a series according to Eq. (33) increases quickly, due to the nested sums of Bessel functions, and the greater number of parameters. So the analytic calculation is only feasible for the most simple form of the input gluon.

4.2 LO gluon fit

Before any definite conclusions can be drawn on the applicability of this approach of Forshaw et al. [15], we have to overcome the restrictions mentioned above. We do this by transforming the moment space expression according to Eq. (31) back to x -space numerically. This allows us to use a conventional form for the gluon which in x -space can be written as

$$x g(x, Q_0^2) = N x^{-\lambda} (1 + \eta x) (1 - x)^\gamma. \quad (36)$$

The resummed gluon is evolved to Q^2 by multiplying this input distribution with R_n and $Z_n(Q^2, Q_0^2)$ according to Eq. (29). An additional advantage of this method is that predictions for F_2 and F_L are obtained simply by multiplying in n -space the appropriate Wilson coefficients with the gluon solution before transforming to x -space numerically.

We can now also exploit the fact that Z_n can be calculated analytically. First note that due to the LO BFKL characteristic equation (13) we can write the measure of the integral as

$$d \ln Q^2 = \frac{4C_A}{\beta_0 n} \frac{d\chi(\gamma_L)}{d\gamma_L} \gamma_L, \quad (37)$$

and thus we can rewrite the integral as [21]

$$Z_n(Q^2, Q_0^2) = \int_{\gamma_L(n, Q_0^2)}^{\gamma_L(n, Q^2)} d\gamma \gamma \frac{d}{d\gamma} \chi(\gamma). \quad (38)$$

But this integral is solved easily using integration by parts

$$\begin{aligned}
\int d\gamma \gamma \frac{d}{d\gamma} \chi(\gamma) &= \gamma[2\gamma_E + \chi(\gamma)] + \ln \frac{\Gamma(\gamma)}{\Gamma(1-\gamma)}, \\
Z_n(Q^2, Q_0^2) &= 2\gamma_E [\gamma_L(n, Q^2) - \gamma_L(n, Q_0^2)] + \\
&+ n \left[\frac{\gamma_L(n, Q^2)}{\bar{\alpha}_s(Q^2)} - \frac{\gamma_L(n, Q_0^2)}{\bar{\alpha}_s(Q_0^2)} \right] + \\
&+ \ln \frac{\Gamma[\gamma_L(n, Q^2)]}{\Gamma[1-\gamma_L(n, Q^2)]} - \ln \frac{\Gamma[\gamma_L(n, Q_0^2)]}{\Gamma[1-\gamma_L(n, Q_0^2)]}.
\end{aligned} \tag{39}$$

This equation can be evaluated numerically once γ_L is known. We find this solution of the characteristic equation by using a complex Newton method using the expansion of the solution (14) as starting value.

We furthermore note that all factors, including the ones stemming from the inversion to x -space, can be conveniently split into a simple product of terms, all depending on n but *only* on one of either x , Q_0^2 or Q^2 . If the n points used for the numerical integration are kept fixed, then one can obtain the results by multiplication of the appropriate combination of the x , Q^2 and Q_0^2 terms calculated in advance. In order to use fixed n points, the integration path is split up into pieces small enough to guarantee unique results. These pieces are evaluated and added one by one until convergence is achieved. We have checked that this method yields the same results as numerical routines using fixed integration path lengths and a self-adapting numerical integration. But our new method is actually even quicker than the “analytical” solution of the last section which of course depends on the numerical evaluation of sums of Bessel functions.

We have tested a large set of fits using the gluon parametrization (36) shown above. The starting scale Q_0^2 was also fitted, but usually this parameter ended up at the upper limit set to the lowest Q^2 of the fitted points. We varied this lowest Q^2 from 2.0 GeV² to 3.5 GeV². Also we tested the effects of including the subleading term, of constraining the small x growth of the background $F_2 \sim x^{-0.08}$ and of constraining the gluon power $xg \sim x^{-\lambda}$ to $0 < \lambda < 2$. The results of the fits to the same data as in the previous section are summarized in Table 2.

$\frac{dC_g}{d\ln Q^2}$ added	$F_2^{bckgr.}$ $\sim x^{-0.08}$	$xg \sim x^{-\lambda}$ $0 < \lambda < 2$	$\chi^2/d.o.f.$ for $Q^2 \geq$				
			2.0 GeV ²	2.5 GeV ²	2.8 GeV ²	3.0 GeV ²	3.5 GeV ²
			3.08	1.72	1.35	1.23	1.00
		•	3.12	1.77	1.41	1.26	1.04
	•		3.17	1.74	1.43	1.26	1.03
	•	•	3.19	1.78	1.48	1.29	1.06
•			2.30	1.02	.679	.625	.583
•		•	2.30	1.02	.680	.626	.583
•	•		2.43	1.33	1.00	.814	.689
•	•	•	2.98	1.33	1.00	.814	.689

Table 2: Fits using the formalism of Forshaw et al. and the general form of the gluon (36). The left part of the table shows the type of fit performed and the right part shows the χ^2 per degree of freedom for different lowest Q^2 of the fitted data.

The fits including the subleading terms $dC_g/d\ln Q^2$ describe the data much better. In spite of this we do not believe that these terms should be included, since they always lead to an obviously wrong behaviour in the small x region at low to medium Q^2 . A typical example is given by the dot-dashed curve in Fig. 3 that also displays other fits of Table 2. It shows the 2.8 GeV² fit of the bottom row in Table 2. The negative contribution of these terms overwhelms the growth of F_2 in the region $\sim 3 - 10$ GeV² at small x . The data constrain the fit, but it starts to fall right after the data point smallest in x . So the negative contribution on the one hand improves the description of the existing data due to a slowed growth, but on the other hand renders any prediction for future data at smaller x impossible.

All the other curves in Fig. 3 correspond to fits without subleading terms, but constrained in F_2 and xg (corresponding to row four in Table 2). For all fits except for the one with $Q^2 \geq 3.5$ GeV², the fitted Q_0^2 equals the lowest Q^2 bin, so that the corresponding curve in that bin shows the F_2 background. The fitted background of the exception is shown separately in the 3.5 GeV² bin.

A general trend is that the fits get worse as lower Q^2 data are included. This is primarily due to the strong growth induced by the BFKL resummed anomalous dimension at low Q^2 . As is obvious by comparing the solid curves at 2.0 GeV^2 and at 2.8 GeV^2 in Fig. 3, the growth at small x is enormous over a short evolution length. Thus the fit forces the background to fall towards smaller x to be able to describe data at higher Q^2 at all. To a lesser extent this is also true for the fits starting at 2.8 and 3.5 GeV^2 . The fit stays below the data at low Q^2 and small x in order to describe the bulk of data at higher Q^2 . Above 12 GeV^2 all fits describe the current small x data well. But if the precision and depth in x of the HERA data continues to improve, this limit may go up.

A few comments on the obtained fit parameters are in order. First the tendency of Q_0^2 to always end up around its highest allowed value is easily explained by the fact that a shorter evolution length inhibits the strong growth somewhat. Considering the fits with subleading terms first, the background is qualitatively $-0.7 + 0.7 \cdot x^{-0.08}$ (if the power of x is constrained), or $0.4 + \mathcal{O}(10^{-3}) \cdot x^{-0.7}$ (for an unconstrained power of x). This shows again that the introduction of the subleading terms leads to pathological consequences at small x , since the “free” background grows strongly in this region to compensate for the fall of the F_2 caused by the evolution.

All fits with subleading terms, except for the one with $Q^2 \geq 2.0 \text{ GeV}^2$, lead to a gluon with parameters of the order $x g \sim 2 \cdot 10^{-3} x^{-1} (1 + 700 x) (1 - x)^{20}$. Basically the same pattern is seen here. The gluon stays very small to inhibit the growth up to the small x region, where it grows rapidly to stop the fall of F_2 . The power of $(1 - x)$ is actually at the allowed limit. If this parameter is left to vary freely, it will even grow to $\mathcal{O}(10^3)$. This basically does not change the small x behaviour, but of course effectively sets the gluon to zero for larger x . The χ^2 is not improved significantly however and thus we can constrain this parameter to stay at least in the region of realistic values. For the $Q^2 \geq 2.0 \text{ GeV}^2$ fit the strong BFKL like growth influences the χ^2 even more and forces $\eta \rightarrow -1$ and a weaker growth. The parameters are then of the order $x g \sim 6 \cdot 10^{-2} x^{-0.6} (1 - x)^{21}$.

Turning to the fits without subleading terms, we find this effect for all gluons, so that they effectively always have $(1-x)^{21}$. If the power of $x^{-\lambda}$ is left constrained, it is always pushed to the upper bound of zero. On releasing it we find $\lambda \sim 0.2$ and the normalization grows to about double its former value, so that the gluon qualitatively has the form $x g \sim 1.8 x^{0.2} (1-x)^{21}$. The fit yields a rather small gluon with flat or even “valence-like” behaviour suited to suppress the growth of F_2 . Since now the fit is not forced anymore to compensate the negative contributions of the subleading terms, the F_2 parameters vary with the different fits. It is interesting to note that the variation of the gluon parameters is small in comparison, hinting that at low Q^2 the influence of the background is strong.

We can conclude that despite some improvement upon using a more general gluon input, the fits still cannot describe the data well if started from low Q^2 scales. Even though the subleading terms lower the χ^2 , a closer look reveals that their influence at small x leads to unphysical results. A word of caution has to be said about the influence of Λ_{QCD} . Lowering it to values as low as the one considered in the original paper [15] can halve the χ^2 of the fit, since the effects of the low starting scales are compensated somewhat. But in adopting such a low value of Λ_{QCD} one basically loses the connection to the large x region completely. If one attempts to vary Λ_{QCD} in fits from low starting scales Q_0^2 , then one sees soon that Λ_{QCD} always drops to the lowest limit set. This would of course not happen if there were large x data constraining the fit. So we here have chosen to fix it at a realistic value instead.

5 Inclusion of the quark sector

We have seen that all attempts to describe the structure function data using only a small x modified gluon density have failed. Thus the next logical step is to incorporate the more or less neglected quark densities. At the same time, we want to stay as close to the successful conventional renormalization group equations as possible. A method to achieve this was suggested by Catani et al. [13] and used in the paper of Ellis et al. [16], but only

by evolving an existing set of parton distributions (MRSD₀, [22]). In the following, we describe this approach briefly and present the results of our fits based on this method.

The basic idea is to take the renormalization group equations in their two-loop-form, and to modify the anomalous dimension matrix according to Eq. (18). The importance of implementing the fundamental energy-momentum conservation for the modified equations has already been stressed in [16]. Energy-momentum is of course always conserved in the conventional formalism. In Mellin space this means that the first moments of the anomalous dimensions have to vanish:

$$\sum_i \gamma_{ij}(n=1) = 0. \quad (40)$$

The all order small x resummations violate this equation and it has to be enforced by hand somehow. Additionally, when we combine the two-loop with the small x expressions, we have to avoid double counting of the leading terms which appear in both the two-loop expressions and the resummed expressions. This can easily be done by simply subtracting the first term in γ_L , and the first two terms in γ_{NL} . As we are now working in next-to-leading order, we have to choose a definite factorization scheme. In the following we will work in the DIS-factorization scheme, since in this scheme there exists a fully resummed expression for γ_{NL} , as mentioned earlier.

Concerning energy-momentum conservation, several ansätze have been suggested in the literature. Ellis et al. [16] used two different ones, a “hard” one where the small x corrections $\gamma_{ij}(n)$ are replaced by $\gamma_{ij}(n) - \gamma_{ij}(1)$, and a “soft” one where these corrections are multiplied with a factor $(1-n)$. Blümlein et al. [23] additionally proposed the “conserving factors” $(1-n)^2$ and $(1-2n+n^3)$. Although these are all arbitrary implementations of the momentum sum rule, one can study with these different factors the possible impact of yet unknown higher order corrections¹. In [23] it was already shown that with these factors it is possible to suppress the small x corrections, or even to overcompensate the

¹Ball and Forte [24] have circumvented the energy-momentum conservation problem in a different way. They used a factorization scheme in which the unknown higher order terms γ_δ , γ_η in the anomalous dimension matrix are *defined* by the momentum sum rule Eq. (40).

expected growth at small x .

There are some theoretical problems associated with these ansatzes. First, we consider the hard implementation. While this does not modify the n -dependence of the resummed corrections at all, it requires their evaluation at $n = 1$. This causes a problem if the starting scale of the evolution is low, since the resummed n -plane pole $n_r = \bar{\alpha}_s 4 \ln 2$ can in this case pass through $n = 1$, making further calculations impossible. For example, the MRS R1 fit [8] uses $\Lambda_{\text{QCD}} = 241 \text{ MeV}$ and a starting scale Q_0^2 of 1 GeV^2 , leading to $n_r = 1$ at $Q^2 = 1.07 \text{ GeV}^2$ using the two-loop formula for α_s . Moreover, the generated structure functions are still much too steep to describe the data, so we will not use it further.

Second, factors involving higher powers of n than n^2 (like one of those in [23]) cause a factorization problem. If we remember that the leading term of γ_{qg} beyond the two-loop expression is proportional to $(\bar{\alpha}_s/n)^2$ (Eq. (26)), such conserving factors imply that γ_{NL} times the conserving factor does not vanish anymore for $n \rightarrow \infty$. This means it cannot be inverted to x -space *on its own*. Since the anomalous dimensions are folded with parton distributions which for reasonable choices of the input fall off better than $1/n$ for $n \rightarrow \infty$, this is not a problem for the evolution program, but it is still an indication that this product is not correctly factorized anymore. For this reason we do not examine even higher powers of n in the conserving factor.

Now we have to comment on our implementation of the resummed expressions into the two-loop evolution program. Since we are using a program which is based on the two-loop analytical solution in moment space of the renormalization group equation [6, 25], this is not as simple as it would be e. g. in a Runge-Kutta based x -space evolution program. Let us first write down the singlet renormalization group equation in the two-loop form including the small x resummations:

$$\frac{d\vec{f}(n, Q^2)}{d\alpha_s} = \left[\frac{\alpha_s}{2\pi} \hat{\gamma}^{(0)}(n) + \left(\frac{\alpha_s}{2\pi} \right)^2 \hat{\gamma}^{(1)}(n) + \hat{\gamma}^{\text{res}}(n, \alpha_s) \right] \frac{1}{-\frac{\beta_0}{4\pi} \alpha_s^2 - \frac{\beta_1}{(4\pi)^2} \alpha_s^3} \vec{f}(n, Q^2) \quad (41)$$

The vector \vec{f} consists of the quark singlet f^s and the gluon density f^g , and we employed

the two-loop equation for α_s :

$$\frac{d\alpha_s(Q^2)}{d\ln Q^2} = -\frac{\beta_0}{4\pi}\alpha_s^2(Q^2) - \frac{\beta_1}{(4\pi)^2}\alpha_s^3(Q^2) \quad (42)$$

with the approximate solution

$$\frac{\alpha_s(Q^2)}{4\pi} = \frac{1}{\beta_0 \ln(Q^2/\Lambda^2)} - \frac{\beta_1 \ln \ln(Q^2/\Lambda^2)}{\beta_0^3 [\ln(Q^2/\Lambda^2)]^2}. \quad (43)$$

The solution of Eq. (41) is not trivial, since we are dealing with a matrix equation; furthermore, it is unclear how to incorporate the resummed expressions involving higher powers of α_s into an approximate solution which is accurate only to $\mathcal{O}(\alpha_s^2)$. We do this by separating the treatment of higher order terms α_s^i , $i \geq 3$ from the resummed terms $\alpha_s (\alpha_s/n)^k$, $k \geq 2$:

$$\begin{aligned} \frac{d\vec{f}(n, Q^2)}{d\alpha_s} = & \left[-\frac{2}{\beta_0 \alpha_s} \left\{ \hat{\gamma}^{(0)}(n) + \frac{\alpha_s}{2\pi} \left(\hat{\gamma}^{(1)}(n) - \frac{\beta_1}{2\beta_0} \hat{\gamma}^{(0)}(n) \right) + \mathcal{O}(\alpha_s^2) \right\} \right. \\ & \left. + \frac{1}{-\frac{\beta_0}{4\pi}\alpha_s^2 - \frac{\beta_1}{(4\pi)^2}\alpha_s^3} \left\{ \hat{\gamma}^{\text{res}}(n, \alpha_s) + \mathcal{O} \left(\alpha_s^2 \left(\frac{\alpha_s}{n} \right)^k \right) \right\} \right] \vec{f}(n, Q^2), \quad (44) \end{aligned}$$

$$\vec{f}(n, Q^2) = \exp \left[-\frac{2}{\beta_0} \hat{\gamma}^{(0)}(n) \ln \frac{\alpha_s(Q^2)}{\alpha_s(Q_0^2)} \right] \quad (45)$$

$$\begin{aligned} & -\frac{1}{\pi \beta_0} (\alpha_s(Q^2) - \alpha_s(Q_0^2)) \left(\hat{\gamma}^{(1)}(n) - \frac{\beta_1}{2\beta_0} \hat{\gamma}^{(0)}(n) \right) \\ & - \int_{\alpha_s(Q_0^2)}^{\alpha_s(Q^2)} d\alpha \frac{\hat{\gamma}^{\text{res}}(n, \alpha_s)}{\frac{\beta_0}{4\pi}\alpha_s^2 + \frac{\beta_1}{(4\pi)^2}\alpha_s^3} + \mathcal{O} \left(\alpha_s^2, \alpha_s^2 \left(\frac{\alpha_s}{n} \right)^k \right) \Big], \quad (46) \end{aligned}$$

with $k \geq 2$. Note that we could expand the denominator of the resummed term as we did for the RG term, since that would only introduce errors of the same order as in the resummation. But this would not simplify the calculation.

Since $\hat{\gamma}^{\text{res}}$ starts with $\alpha_s (\alpha_s/n)^2$ after subtraction to avoid double counting, the leading power of the integral is $(\alpha_s/n)^2$. In expanding the matrix exponential we would encounter commutators of all three terms. But the commutator of the conventional NLO term with the resummation integral is suppressed by α_s . This contribution would be of the same order as the commutator of the *error* of the resummation with the LO RG term and can

be ignored. Thus we can attach all the resummed terms to $\hat{\gamma}^{(1)}$ via

$$\hat{\gamma}^{(1,\text{res})}(n, \alpha_s) = \hat{\gamma}^{(1)}(n) + \frac{\pi\beta_0}{\alpha_s(Q^2) - \alpha_s(Q_0^2)} \int_{\alpha_s(Q_0^2)}^{\alpha_s(Q^2)} d\alpha \frac{\hat{\gamma}^{\text{res}}(n, \alpha)}{\frac{\beta_0}{4\pi}\alpha^2 + \frac{\beta_1}{(4\pi)^2}\alpha^3}. \quad (47)$$

For the final solution we then treat the resummed anomalous dimension $\hat{\gamma}^{(1,\text{res})}$ exactly like the original $\hat{\gamma}^{(1)}$. The exponential of the matrices is expanded and terms of $\mathcal{O}(\alpha_s^2)$ not stemming from the resummation are dropped. Thus, concerning the resummed terms, the solution is accurate up to $\mathcal{O}(\alpha_s^2 (\alpha_s/n)^k)$ consistent with the error inherent to the resummation itself.

We have checked that using this procedure we can reproduce the results of [16]. But we want to improve on the results shown there by on the one hand refitting the input parton distributions and on the other hand by lowering the starting scale Q_0^2 to values used in recent conventional RGE fits. We expect that lowering the starting scale leads to the same kind of problems as encountered in the previous sections, namely a steep growth in the region of small x . Thus it is necessary to refit the parton distributions to test if one can compensate this growth.

In principle one should do a fit to all relevant data to constrain the (presumably) universal new input parton densities and α_s as much as possible. Then the analysis would be truly competitive to conventional RGE analyses like [8, 9]. But the small x resummations for most of the processes are unknown. Furthermore the computing time would be prohibitive due to the more complicated expressions. Even if we just concentrate on F_2 , the calculations are already rather time consuming.

Thus we take the following approach: we use the optimal MRS R1 conventional RGE fit [8] as our starting point. The ansatz for the input parton distributions can be found there. We assume that at large x the new parton distributions would be similar to the R1 ones, since the resummation effects should be small at large x and since there are many experiments constraining the parton distributions in this region. In practice we calculate the original R1 partons and F_2 at $x = 0.05, 0.15, 0.4$ and compare them to the new fit using an artificial error of one percent. This assumed small error is necessary to force the

fit to match the large x region, since as we will see the small x region is not well described and would overwhelm any weak constraint at large x . The valence quark distributions are not directly affected by the small x resummations. They could be influenced indirectly by trading momentum with the quark sea, but they are well constrained by experiments and negligible in the region of small x . In order to save computing time we do not fit the parameters of the valence quark input, but keep them fixed at the R1 values. We also keep the value of Λ_{QCD} fixed, since it is mainly constrained by experiments in the large x region as discussed in [8].

We allow for an additional degree of freedom by fitting $\lambda_{\Delta}^{\text{MRSR}} \equiv -0.3$ of $x\Delta \equiv x(\bar{d} - \bar{u}) \sim x^{-\lambda_{\Delta}}$. The correct $u - d$ flavour symmetry breaking is taken care of by the large x constraints of the sea. The glue and the sea are now fitted at $x < 5 \cdot 10^{-2}$ to the data. Of course in this region the HERA data [1, 2, 3] are dominant. Fitting to the whole bulk of HERA data would again be too time consuming. So instead we use the R1 fit, which describes HERA data very well, to generate F_2 data points in the x range that is covered by HERA. The errors are adjusted to match those of the experiment. Finally it should be mentioned that the appropriate adjustments of the parton distributions due to the scheme change $\overline{\text{MS}} \rightarrow \text{DIS}^{\text{res}}$ have to be made². This is done automatically at the starting scale Q_0^2 , so that only the input distributions are affected. Since we are mainly interested in how the parameters are changed when the small x resummations are switched on and since we keep the valence quarks fixed, only the conventional Wilson coefficients are used for the transformation. This does not limit the fits, but the obtained parameters should not be used for a direct $\overline{\text{MS}}^{\text{res}}$ calculation.

Let us mention that in the previous fits by Ball and Forte [24, 26] only the small x powers $\sim x^{-\lambda}$ of the glue and sea were refitted. We have found that the large x behaviour of the partons can be reproduced by rearranging the various large x parameters, so that for example the normalization can change. This does of course affect the small x region as well, so that we find it necessary to fit the complete ansatz. Also they introduce a

²The superscript “res” merely signifies the inclusion of the small x resummations, not a change of the scheme definition.

“reference value” x_0 above which all resummed expressions are switched off. Although their motivation to separate the large from the small x region is clear, we see no need in the formalism to introduce such an arbitrary scale. Nevertheless, their conclusions are quite similar to ours, since in a later paper [26] x_0 is found to be almost zero, thus excluding any need for small x resummed expressions in the evolution equations. So we will basically confirm their results with our different and in some aspects more general method.

To see the influence of the resummation on the parton densities we show in Fig. 4 the ratio of the resummed gluon and quark singlet to the standard one. As expected the ratio goes to one for large x , but the expected slower convergence of the sea curves is also clearly visible. For larger Q^2 the influence of the resummation is much reduced. Most of the difference is picked up at low Q^2 values which is understandable considering the moving resummed pole. To test the impact of yet unknown higher order contributions as mimicked by our conserving factors, we are especially interested in the first term $\sim n$; but changing its coefficient requires the inclusion of higher powers of n . Comparing the $(1 - 2n + n^2)$ and $(1 - 2n + n^3)$ curves, we see that their influence is strong. In the latter case, the partons are even *smaller* than the standard ones and a fit using this factor leads to an unacceptable *fall* of F_2 in the small x region. Thus it is evident that present small x resummations have no predictive power.

On the other hand we have already mentioned that exactly the term $\sim n^3$ and all even higher powers spoil the transformation back to x space. If we require the anomalous dimensions to be transformable, the maximum power allowed for the conserving factor is n^2 . In combination with the strong large x constraints we then always get partons and F_2 larger than the ones obtained by conventional NLO evolution. We checked this by fitting the conserving factor as well, i. e. we fitted a of $(1 - a \cdot n + b \cdot n^2)$ with $b = a - 1$. The fit gives $a = 1.2944$ and satisfies the large x constraints well, but the $(1 - n)^2$ curve does better in the small x region. Actually if we *only* fit a and leave all other parameters at their original MRS R1 value, we get $a = 1.2651$. So for these values of a the effect of the

small x resummations at large x seems to be minimized.

Such large effects from subleading terms are caused by the resummed BFKL pole. For $Q_0^2 = 1 \text{ GeV}^2$ it lies around $n_r \simeq 1$. So considering a contour close to the resummed pole we see that the main contribution of the resummed pole comes for regions of n where the change $n^2 \rightarrow n^3$ in the conserving factor means a considerable change of the subleading terms. Of course this depends on the starting scale Q_0^2 as well, for example at $Q_0^2 = 4 \text{ GeV}^2$ we have $n_r \simeq 0.7$. So on top of the change of the resummation itself the relative importance of the subleading terms will change. This arbitrariness is just a sign of our ignorance concerning the subleading terms, but at least we can exclude powers of n higher than two from the conserving factor to avoid picking up terms that will not occur in the real subleading expressions.

The results for the partons translate directly to $F_2(x, Q^2)$ shown in Fig. 5. As expected the resummed calculations always overshoot the data at small x . The influence of the terms down by one power in n is strong as can be seen by the spread in the curves. The “dips” in the curves are somewhat artificial, basically they are due to the too strong rise of the calculated F_2 compared to the data. Then χ^2 is minimized by adjusting the partons so that the curves are below the data at larger x first. Even the curve using the $(1 - n)^2$ factor is too steep at small x ; this is even more true for the other curves. The curve with the fitted conserving factor $a = 1.2944$ mainly leads to an optimal large x behaviour. It is interesting to note that if we leave out all large x constraints and fit the conserving factor, we get a good description ($\chi^2/\text{d.o.f.} \simeq 1$) of the small x data for $a = 2$. But then at larger x we are totally off the F_2 and parton constraints. Due to the coincidence that the fitted a for the best small x description is close to the $(1 - n)^2$ we tested for the complete fit, we can claim that the $(1 - n)^2$ curve is basically the best if one wants to describe *all* F_2 data but emphasizes the small x region.

A problem of all fits has to be mentioned. If we leave Λ_{QCD} as a free parameter it always drops to low values. Despite the still large errors on Λ_{QCD} and despite the fact

$x [g S \Delta](x, Q_0^2) =$ $Ax^{-\lambda}(1-x)^\eta(1+\epsilon\sqrt{x}+\gamma x)$		RGE	Resummed	
		MRS R1	$(1-n)^2$	$a = 1.2944$
Gluon	(A_g)	24.5	0.94777	36.1
	λ_g	-0.41	0.26536	-0.547
	η_g	6.54	3.9801	6.866
	ϵ_g	-4.64	-1.5297	-4.483
	γ_g	6.55	4.2279	6.135
Sea $(\epsilon_\Delta = 0, \eta_\Delta = \eta_S)$	A_S	0.42	0.41647	4.801
	λ_S	0.14	0.036837	-0.3928
	η_S	9.04	10.873	8.815
	ϵ_S	1.11	5.1104	-0.330
	γ_S	15.5	22.073	0.441
	A_Δ	0.39	0.084878	0.001299
	λ_Δ	-0.3	-0.59879	-0.1086
	γ_Δ	64.9	72.461	1473
$\frac{\chi^2}{\text{d.o.f.}}(F_2), x < 5 \cdot 10^{-2}$			1.88	11.7
$\frac{\chi^2}{\text{d.o.f.}}(F_2, \text{partons}), x \geq 5 \cdot 10^{-2}$			126	6.21

Table 3: The fitted partons using RGE plus small x resummations in comparison with the original RGE MRS R1 partons [8].

that in principle all determinations of α_s should incorporate small x resummations to be consistent, we believe that $\Lambda_{\text{QCD}}^{n_f=4} \simeq 200$ MeV should be taken as typical for a “low” α_s . Experimentally low values of α_s stem from data at large x [27] where resummation effects should be small, so we expect that this holds true in the cases considered here. The effect of lowering Λ_{QCD} is of course greatest for the largest resummation effects, so we show a curve with the conserving factor $(1-n)$ and $\Lambda_{\text{QCD}}^{n_f=4} = 200$ MeV. The $\chi^2/\text{d.o.f.}$ at small x is for the lower Λ_{QCD} reduced from 21 to 11. A straight fit would yield $\Lambda_{\text{QCD}}^{n_f=4} = 180$ MeV, but this value should not be taken too seriously, since it depends on how strictly we implement the large x constraints.

In Table 3 we show the parameters of those two fits that can be considered optimal. A_g is calculated via the momentum sum rule and $\Lambda_{\text{QCD}}^{n_f=4} = 241$ MeV. $S \equiv 2(\bar{u} + \bar{d} + \bar{s})$ is the total sea quark distribution, and $\Delta \equiv \bar{d} - \bar{u}$; for further details and the valence distributions refer to [8]. The choices for the conserving factor giving the best small x behaviour $(1 - n)^2$ or the best large x behaviour $(1 - 1.2944 n + 0.2944 n^2)$ are shown. If one is mainly interested in describing the small x region, one should use the $(1 - n)^2$ conserving factor. But then in the large x region the RGE partons are not reproduced well. The χ^2 here is dominated by the partons constrained by an artificial one percent error. A more realistic choice of a five to ten times bigger error would of course reduce the χ^2 considerably. But we see that even at small x the quality of the conventional RGE fit is not matched. Most of the χ^2 comes here from the points with smallest x at the lower Q^2 bins. Looking at the parameters we see that the input sea has turned flat whereas the input gluon is now growing with smaller x instead of being valence like. The normalization of the gluon is lowered correspondingly.

The input sea of the $a = 1.2944$ fit has become valence like. The gluon has stayed more or less the same. On the one hand we see that the fit cannot describe the small x data at all. On the other hand at large x the MRS R1 partons and F_2 are reproduced well. We can be sure that this fit would be compatible with experimental data at large x . Due to the necessary artificial constraint at large x it makes no sense to add the χ^2 for all x , so one cannot conclude that the $a = 1.2944$ is the overall better fit. A more sophisticated treatment of the large x region would be needed to determine a true best fit. But since there are still parts of the NLO small x resummation missing and since the conserving factors give just an estimate of the influence of subleading terms, we feel that not much could be gained by improving the large x treatment for the time being.

6 General Discussion

Figure 6 presents a different look at our results. Here we show $\lambda \equiv \partial \ln F_2 / \partial \ln(1/x)$ as determined by the H1 experiment [3] in comparison with theory. To obtain λ a fit of the type $C x^{-\lambda}$ is made for $x < 0.1$ for the H1 data. This should be understood as a cut, so that the actual highest and lowest x value used depends on the data. The two conventional NLO RGE calculations MRS R1 [8] and GRV '94 [28] have been treated by us in a similar way using the same highest x values but extending the lowest x to 10^{-5} . We see the perfect match of the MRS R1 fit, and show for comparison the dynamical GRV '94 [28] predictions which, however, are sensitive to the precise choice of the input scale.

We also show in Fig. 6 the slope predicted by the pure LO BFKL evolution. For this we simply used the λ of our parametrization [10]. For the “resummed” calculations presented in the last sections we again used the fitting method to obtain λ . But the double logarithmic plots of F_2 in Fig. 5 suggests that we have to lower the starting x of our curves. So to avoid the “dips” of the curves presented in this section we use a $x < 10^{-3}$ cut and for the ones of the previous section we even have to use $x < 3 \cdot 10^{-4}$. We show in Fig. 6 λ for all starting scales Q_0^2 of the fits displayed in Fig. 3 and for the different fits displayed in Fig. 5.

We see that the big spread in the predicted λ for all the BFKL inspired methods is diminishing towards higher Q^2 . *But* it lies always above the data except perhaps at very high Q^2 . So the resummed F_2 is always growing too fast in the small x region, since at very large Q^2 the conventional RGE terms are expected to become dominant. This is also probably the explanation why the pure LO BFKL λ is the only one that keeps growing. There are no conventional RGE terms that can take over at high Q^2 for this curve. An interesting feature is that shifting $\Lambda_{\text{QCD}}^{n_f=4}$ from 241 MeV to 200 MeV for the $(1-n)$ conserving factor simply resulted in lowering of λ by about 7.8 percent. If we naïvely interpret this as the ratio of the resummed BFKL poles at $\overline{\alpha_s} 4 \ln 2$, we get

an effective probing scale of 3 GeV^2 . The fact that the LO resummed calculations give predictions for λ that are in the same ballpark as those including additionally the NLO resummations can be attributed to the dominance of the BFKL pole.

The failure of the pure LO BFKL formalism to describe the experimental F_2 data is not so surprising. There has never been any guarantee that the resummation of only the leading logarithms in x would be appropriate in the kinematic region explored by current experiments. We are also forced to introduce three parameters in practical calculations. This is due to our limited understanding of the IR region and of the inclusion of the running coupling. It is a nice feature of the strong BFKL pole that despite these difficulties we can come to the conclusion that LO BFKL is ruled out by experiment at currently accessible small x .

The inclusion of a larger part of the total contributions of perturbative QCD should naïvely lead to a better description of the data. Our calculations using the methods of Forshaw et al. show us clearly that it is not sufficient to use just gluons and the LO resummed anomalous dimensions in RGE type calculations. Since this method is closest to the pure LO BFKL evolution, this result comes as no surprise. So the most promising method should be to use all that is known: the NLO RGE and the LO and part of the NLO resummations in x . In doing so we immediately encounter the first hint of trouble. The resummations in x always violate the fundamental energy-momentum sum rule.

We have to force the evolution to obey this constraint. This means that we can really only rely on the calculations if the results are not changed much when we implement this constraint in various ways. In fact the results depend strongly on how we implement energy-momentum conservation and thus one cannot give reliable predictions for F_2 at small x at all. We have seen that this failure is again due to the strong BFKL pole. The main contribution of it stems from rather large n and thus variations in the conserving factor lead to changes that are formally subleading but numerically important. If we limit our calculations to conserving factors that do not introduce terms absent from higher order

anomalous dimensions, then we can still see a trend in the predictions: again F_2 grows too strongly at small x .

Our results could be taken as an indication that the still missing NLO resummation pieces will not be sufficient to improve the stability of the calculation and its outcome. This would prove that the small x resummations do not lead to a stable perturbative series in contrast to the RG calculations. Of course this is entirely possible, but it would question all future work on this subject. But there are some important caveats concerning such a strong conclusion.

A strong growth that can not be suppressed by adjusting the parton distributions is only encountered if the starting scale Q_0^2 is below approximately 3 GeV^2 . To a lesser extent the variations induced by different conserving factors increase for lower starting scales. Also the fits can always be improved significantly by lowering Λ_{QCD} . Only a true fit to all the large x data would tell us if Λ_{QCD} can be determined uniquely and if the small x region is well described with the value obtained. But our fits already indicate that probably this would not be the case. These problems are all connected to the strong BFKL pole, since the fits always improve if α_s becomes smaller and the pole moves to the left in the n -plane.

It has to be mentioned as well that some closely related calculations do not seem to encounter these problems. The “physical anomalous dimensions” calculations [29, 30] relate only physical observables F_2 and F_L and thus any factorization scheme dependence is avoided. This fit to the data even seems to be preferred over conventional RG calculations. We note that due to the relative order $F_L \sim \alpha_s F_2$ such calculations should be limited to leading logarithms until the next-to-next-to-leading piece of the coefficient functions of F_L is determined. This fit also implies a rather low (LO, 4 flavours) $\Lambda_{\text{QCD}} = 100 \text{ MeV}$. The input scale of the evolution Q_0^2 is determined as 40 GeV^2 and the fit becomes uncompetitive even above 3 GeV^2 . Finally a new scale A_{LL} is introduced at which the “inputs become nonperturbative” [29]. The usual choice $A_{LL} = Q_0^2$ would simplify the formulae

used considerably. But this would spoil the agreement with data, since Q_0^2 would be low.

We suspect that if this kind of fit was redone starting from a low scale $Q_0^2 = A_{LL}$, then the same kind of problems as we have encountered would occur. Calculations using the colour dipole model are also giving good agreement with recent F_2 HERA data [31], but note that they only used a *fixed* strong coupling. Another successful approach [32] based on the CCFM equation [14, 33], does not include the quark sector, uses approximations only valid at small x and represents a LO resummation. But the imposition of a purely kinematic constraint on the gluon ladder introduced in [32] suggests that higher order terms could suppress the growth in the gluon sector.

7 Conclusions

We have used BFKL inspired methods of increasing complexity to obtain predictions for F_2 . The pure LO BFKL evolution is now definitely ruled out by the precise HERA data at small x . Next we turned to combinations of the successful conventional RGE methods supplemented by small x resummations. We have found that the simplest approach, just using gluons and the LO small x resummed anomalous dimensions, fails as well, if we compare it with current small x data. This is especially true if the starting scale Q_0^2 is lowered and can not be avoided by fitting a realistic gluon input distribution. On the other hand lowering Λ_{QCD} a lot improves always the fits significantly, but then the fit of course becomes incompatible with large x data.

Finally we used an ordinary two-loop calculation supplemented by LO and NLO small x resummations starting from a complete set of input parton distributions in a fit to F_2 data over the whole accessible x range. The fundamental energy-momentum sum rule was (arbitrarily) implemented using different conserving factors. Although the use of different conserving factors led to strong variations of the F_2 predictions, we still come to the same conclusions: At small x the growth of F_2 is too strong, but this depends

again on the starting scale Q_0^2 and on Λ_{QCD} . Using current experimental data, only small x resummed calculations starting from low scales $Q_0^2 \sim 1 - 2 \text{ GeV}^2$ can be excluded. Also lowering Λ_{QCD} improves the fit, unless strong large x constraints are implemented. We also see that fitting the input distributions and adjusting the conserving factor only results in shifting the strong BFKL growth to smaller values of x . If no such growth is seen in the experimental data, this would be a definite sign of the absence of BFKL-like contributions.

For a final judgment on the small x resummations we will have to wait until the calculation of the NLO pieces will be completed. Also it is probable that with a starting scale of around 4 GeV^2 it will not be possible to rule out such contributions. Only a true fit to all the usual data using small x resummations consistently will tell us if the assumption that Λ_{QCD} can not be lowered too much because of the large x region is correct. Keeping this in mind, we suggest that currently available methods and data strongly favour conventional RG calculations. If this statement survives the test of time, it will mean that the small x resummations do not represent a good perturbative series. This would shed doubt on all calculations involving them.

Acknowledgments: We thank E. Reya for his advice and A. Vogt for interesting discussions on the conserving factors. This work has been supported in part by the 'Bundesministerium für Bildung, Wissenschaft, Forschung und Technologie', Bonn.

References

- [1] H1 Coll., I. Abt *et al.*, Nucl. Phys. **B407** (1993) 515; ZEUS Coll., M. Derrick *et al.*, Phys. Lett. **B316** (1993) 412.
- [2] H1 Coll., T. Ahmed *et al.*, Nucl. Phys. **B439** (1995) 471; ZEUS Coll., M. Derrick *et al.*, Z. Phys. **C65** (1995) 379.
- [3] ZEUS Coll., M. Derrick *et al.*, Z. Phys. **C69** (1996) 607; H1 Coll., S. Aid *et al.*, Nucl. Phys. **B470** (1996) 3; ZEUS Coll., M. Derrick *et al.*, DESY preprint DESY-96-076.
- [4] E. A. Kuraev, L. N. Lipatov and V. Fadin, Zh. Eksp. Teor. Fiz. **72** (1977) 377 [Sov. Phys. JETP **45** (1977) 199]; Ya. Ya. Balitskij and L. N. Lipatov, Yad. Fiz. **28** (1978) 1597 [Sov. J. Nucl. Phys. **28** (1978) 822].
- [5] G. Altarelli and G. Parisi, Nucl. Phys. **B126** (1977) 298; Yu. L. Dokshitzer, Zh. Eksp. Teor. Fiz. **73** (1977) 1216 [Sov. Phys. JETP **46** (1977) 641].
- [6] M. Glück, E. Reya and A. Vogt, Z. Phys. **C48** (1990) 471.
- [7] M. Glück, E. Reya and A. Vogt, Z. Phys. **C53** (1992) 127 and Phys. Lett. **B306** (1993) 391; M. Glück, E. Reya and M. Stratmann, Nucl. Phys. **B422** (1994) 37; M. Glück, E. Reya and A. Vogt, Z. Phys. **C67** (1995) 433.
- [8] A. D. Martin, W. J. Stirling and R. G. Roberts, Phys. Lett. **B387** (1996) 419.
- [9] H. L. Lai *et al.*, Phys. Rev. **D55** (1997) 1280.
- [10] I. Bojak and M. Ernst, Phys. Rev. **D53** (1996) 80.
- [11] A. J. Askew, J. Kwieciński, A. D. Martin and P. J. Sutton, Phys. Rev. **D49** (1994) 4402; A. J. Askew, J. Kwieciński, A. D. Martin and P. J. Sutton, Mod. Phys. Lett. **A8**, No. 40, (1993) 3813.
- [12] S. Catani, M. Ciafaloni and F. Hautmann, Phys. Lett. **B242** (1990) 47.

- [13] S. Catani and F. Hautmann, Nucl. Phys. **B427** (1994); S. Catani, M. Ciafaloni and F. Hautmann, Nucl. Phys. **B366** (1991) 135.
- [14] S. Catani, F. Fiorani and G. Marchesini, Nucl. Phys. **B336** (1990) 18; M. Ciafaloni, Nucl. Phys. **B296** (1988) 49.
- [15] J. R. Forshaw, R. G. Roberts and R. S. Thorne, Phys. Lett. **B356** (1995) 79.
- [16] R. K. Ellis, F. Hautmann and B. R. Webber, Phys. Lett. **B348** (1995) 582.
- [17] I. Bojak and M. Ernst, University of Dortmund preprint DO-TH 96/18, to be published in Phys. Lett. **B**.
- [18] A. J. Askew, J. Kwieciński, A. D. Martin and P. J. Sutton, Phys. Rev. **D47** (1993) 3775.
- [19] A. D. Martin, W. J. Stirling and R. G. Roberts, Phys. Rev. **D47** (1993) 867; P. J. Sutton, *private communication*.
- [20] E665 Coll., M. R. Adams *et al.*, Phys. Rev. **D54** (1996) 3006.
- [21] J. C. Collins and R. K. Ellis, Nucl. Phys. **B360** (1991) 3.
- [22] A. D. Martin, W. J. Stirling and R. G. Roberts, Phys. Lett. **B306** (1993) 145.
- [23] J. Blümlein and A. Vogt, Acta Phys. Pol. **B27** (1996) 1309; J. Blümlein, S. Riemersma and A. Vogt, Nucl. Phys. **B** (Proc. Suppl.) **51C** (1996) 30.
- [24] R. D. Ball and S. Forte, Phys. Lett. **B358** (1995) 365.
- [25] W. Furmanski and R. Petronzio, Z. Phys. **C11** (1982) 293; M. Diemoz, F. Ferroni, E. Longo and G. Martinelli, Z. Phys. **C39** (1983) 21.
- [26] R. D. Ball and S. Forte, University of Edinburgh preprint 96/14 or DFTT 35/96, July 1996.
- [27] Particle Data Group (R. M. Barnett et al.), Phys. Rev. **D54** (1996) 1.

- [28] M. Glück, E. Reya and A. Vogt, Z. Phys. **C67** (1995) 433.
- [29] R. S. Thorne, Phys. Lett. **B392** (1997) 463 and Rutherford Appleton Laboratory preprint RAL-96-065, January 1997.
- [30] S. Catani, University of Florence preprint DFF 248/4/96, April 1996.
- [31] H. Navelet et al., Phys. Lett. **B385** (1996) 357.
- [32] J. Kwieciński, A. D. Martin and P. J. Sutton, Phys. Rev. **D53** (1996) 6094; A. D. Martin, J. Kwiecinski and P. J. Sutton, Z. Phys. **C71** (1996) 585.
- [33] G. Marchesini, Nucl. Phys. **B445** (1995) 49; S. Catani, F. Fiorani and G. Marchesini, Phys. Lett. **B234** (1990) 339.

Figure Captions

Fig. 1 Comparison of BFKL-evolved structure functions with data from HERA [2, 3] and the E665 [20] experiment. The dashed curves show the soft pomeron background $C_P x^{-0.08}$ fitted for each Q^2 -bin, if C_P greater than zero. Additionally, the MRS R1 RGE fit [8] is shown for illustration.

Fig. 2 Structure function obtained with the analytic prescription of Forshaw et al. [15], with refitted parameters according to the shown data from HERA [2, 3] and E665 [20]. The solid curve is calculated without the subleading term $\partial C_2^g / \partial \ln Q^2$, whereas the others curves include them, with two different choices of Λ_{QCD} .

Fig. 3 Fits to F_2 data as in Fig. 2 but using the gluon in Eq. (35). The lower Q^2 cut of the fitted data is varied and the fitted starting scale Q_0^2 ends up at this value except for the fit $Q^2 \geq 3.5 \text{ GeV}^2$. For this fit the background at $Q_0^2 = 3.36 \text{ GeV}^2$ is displayed in the 3.5 GeV^2 bin. The dot-dashed curve is an example of a fit including subleading terms.

Fig. 4 Impact of the resummed terms in the evolution equation on the singlet (left) and gluon part (right) relative to conventional two-loop calculations. Also the influence of different methods to restore energy-momentum conservation is shown. The unmodified MRS R1 distributions [8] are used as input.

Fig. 5 The results for F_2 of fits using different conserving factors in a NLO calculation including small x resummations. The data used for the fit is shown as stars and experimental data as in Fig. 1 is shown for comparison.

Fig. 6 The slope of F_2 of the calculations using small x resummations compared with experimental data and two conventional NLO RGE calculations. Results of the same method are shown in one line style. The main parameter varied to obtain the different curves of one method is displayed at the curve.

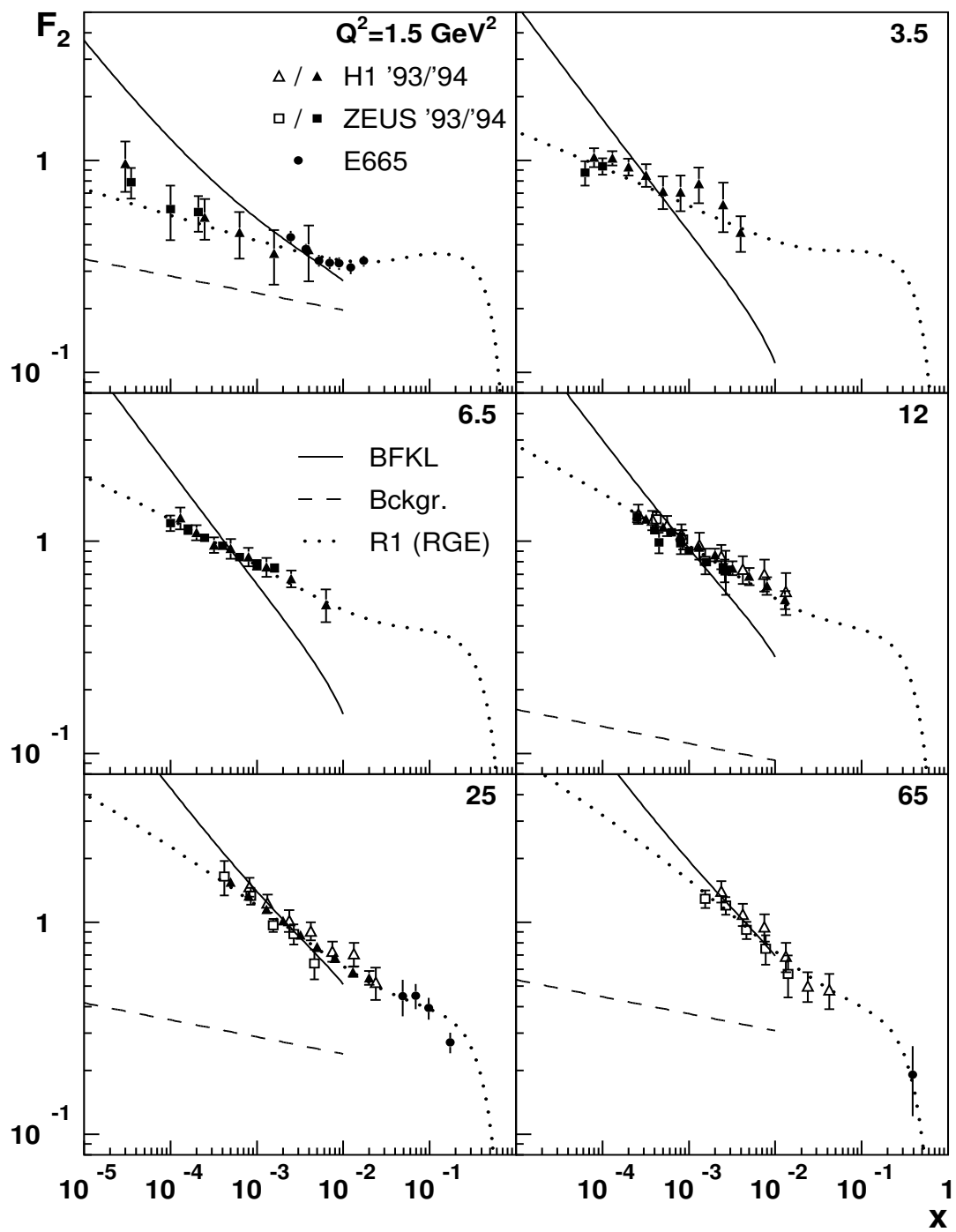


Fig. 1

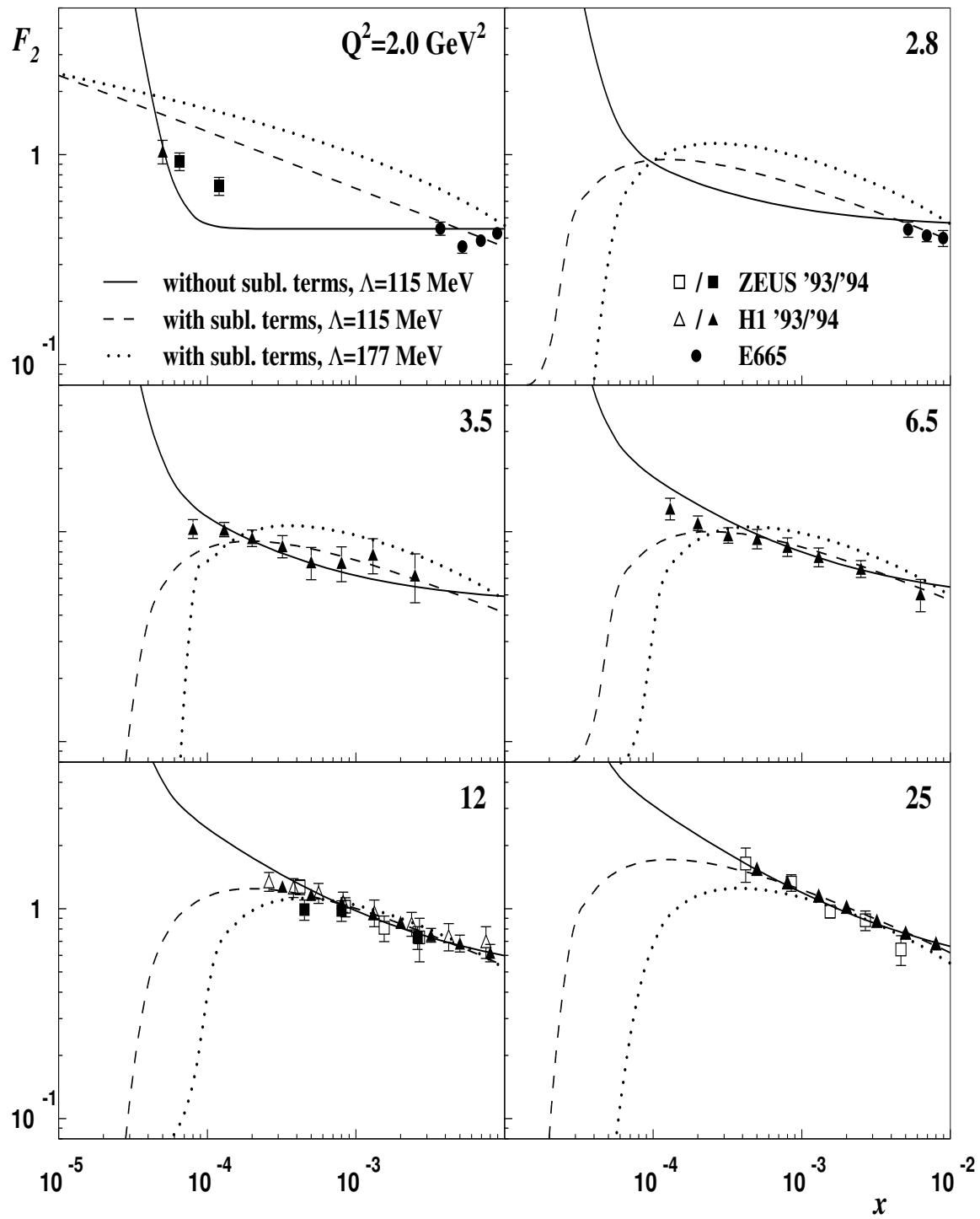


Fig. 2

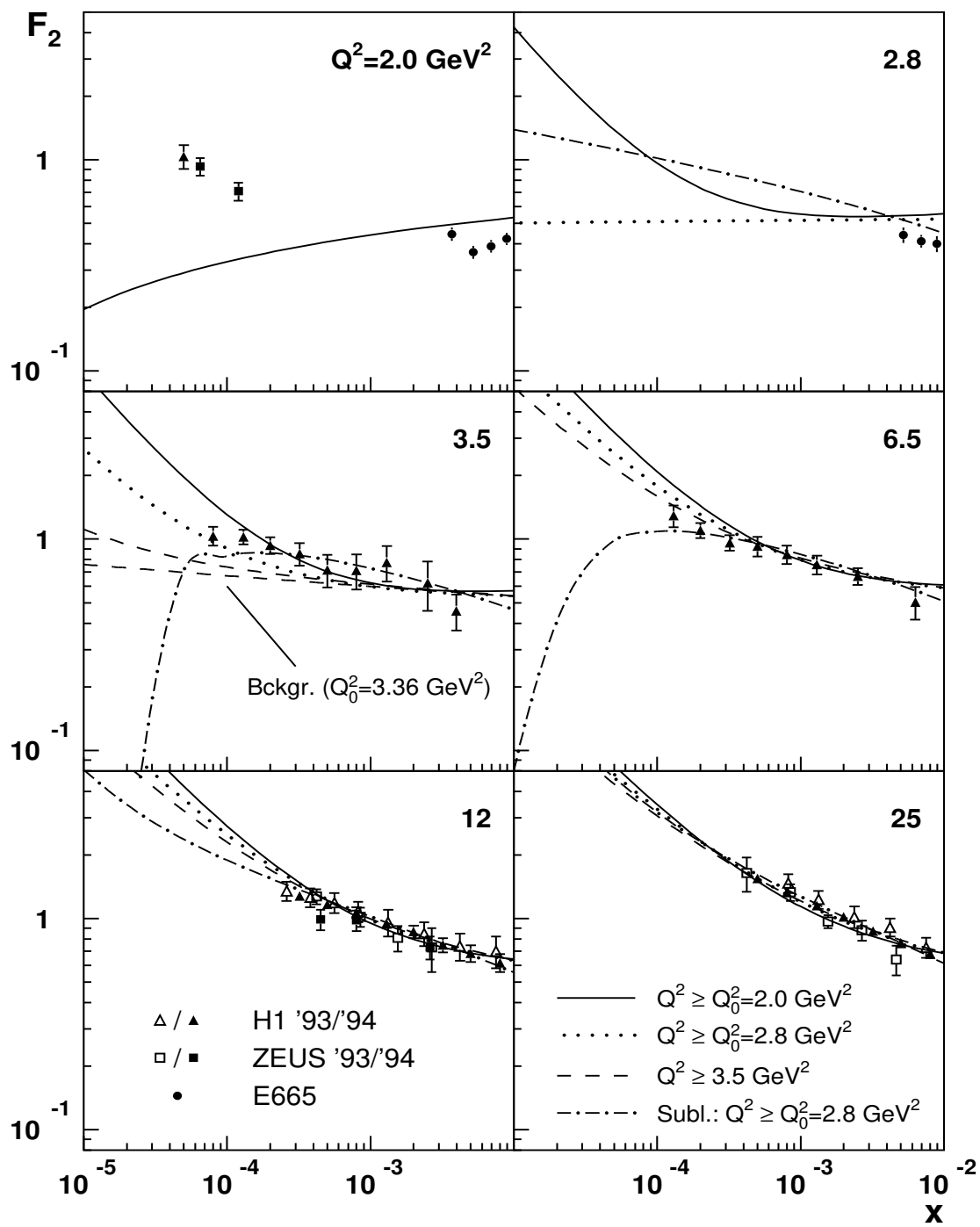


Fig. 3

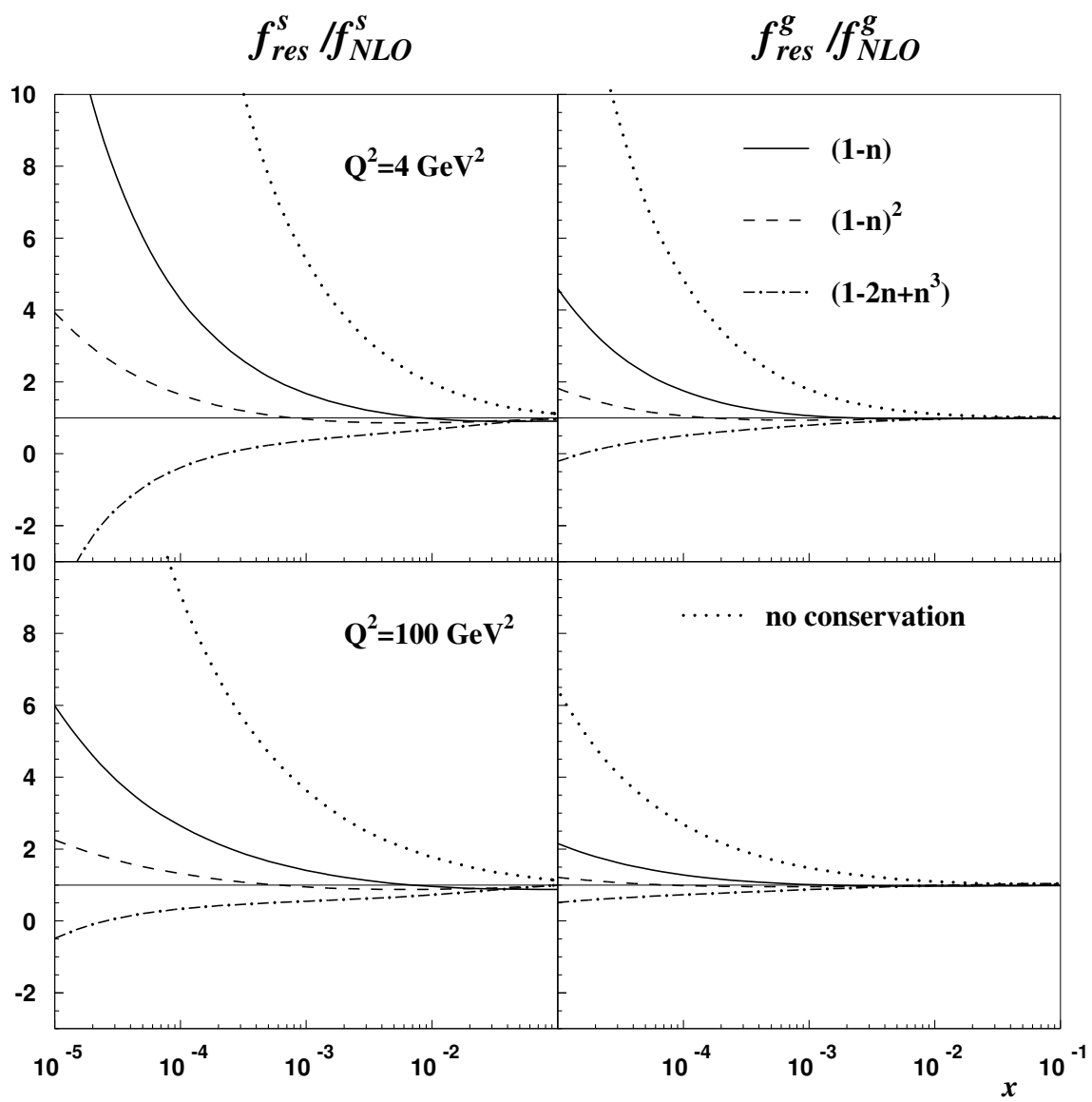


Fig. 4

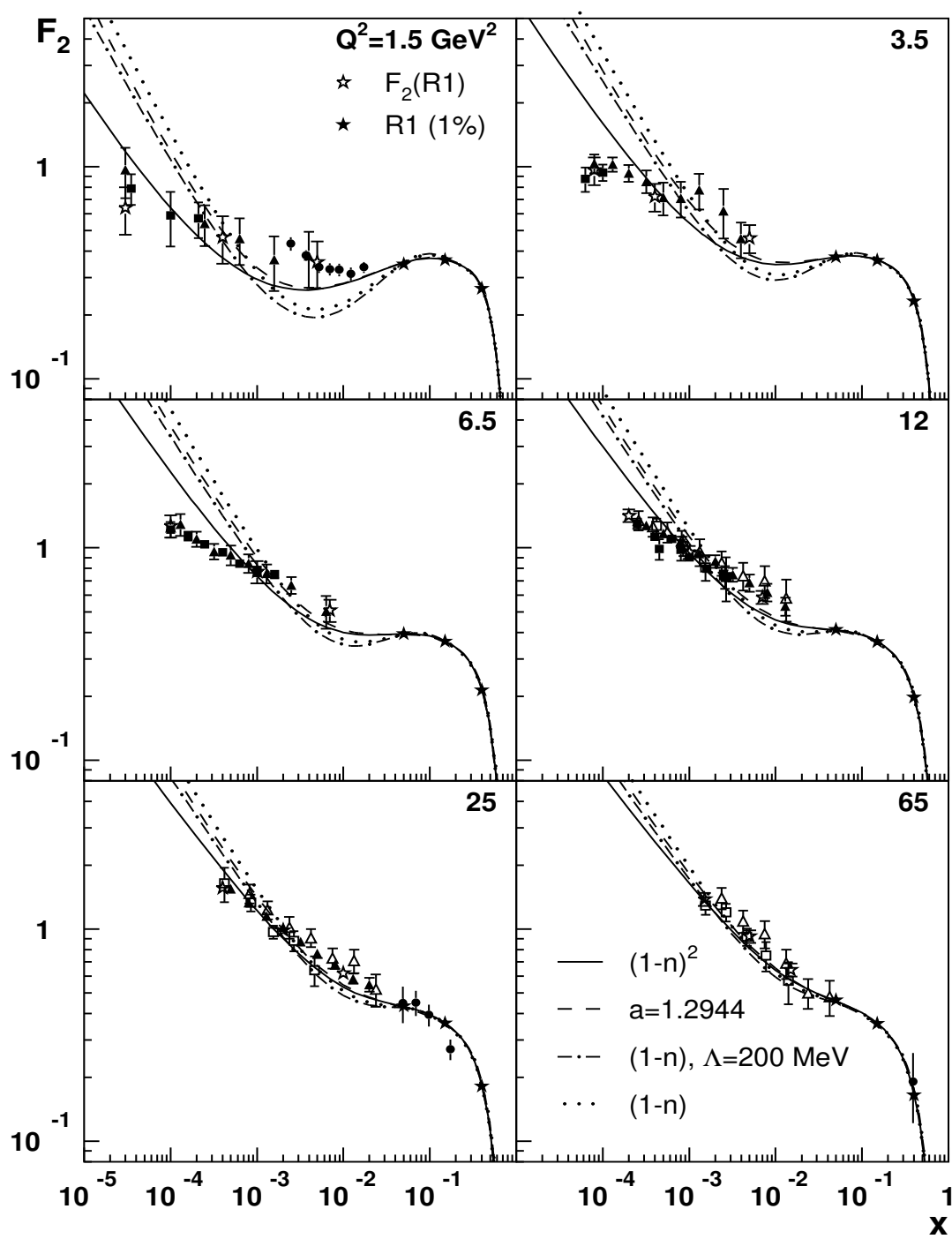


Fig. 5

Fig. 6

